

# A Full Analytic Treatment of Reversible Linear-Scan Voltammetry with Square-Wave Modulation

Keith B. Oldham,<sup>\*,†</sup> David J. Gavaghan,<sup>‡</sup> and Alan M. Bond

School of Chemistry, Monash University, Clayton, Victoria 3800, Australia

Received: July 23, 2001; In Final Form: October 20, 2001

The effect upon reversible linear-potential-scan voltammetry of adding a modulating square wave of any amplitude is examined by solving the governing equations exactly. This solution explains the origin of the “splitting effect” that had previously been observed empirically in the dc component. The ac component is derived in both the time domain and the frequency domain. In the former, it consists of a periodic function, displaying spikes whenever the square wave experiences a sign change. In the frequency domain, harmonics that possess odd multiples of the square wave’s frequency are present, phase shifted by 45°. The dependence of the accurate amplitude on the dc potential and on the square wave’s amplitude is formulated. Comparisons are made with a recent simulative and experimental study of the same system.

## Introduction

Perhaps the most familiar shape to an electrochemist is that generated by plotting current versus time (or potential) when a ramped voltage signal is applied to an electrode at which a reversible electron transfer occurs between solution-soluble species under conditions which are standard in voltammetry. Such a linear-potential-scan voltammogram was initially described in 1948 by Randles<sup>1</sup> and independently by Sevcik.<sup>2</sup> An accurate theoretical treatment of linear-scan voltammetry was first provided by the seminal numerical work of Nicholson and Shain<sup>3</sup> in 1964, for reactions of various degrees of activation polarization, while a fully analytic treatment<sup>4</sup> followed for reversible systems in 1979. The voltammogram is asymmetrically peaked and a complicated expression, presented in eq 15 below, is needed to describe it mathematically. We shall refer to such a voltammogram, which is illustrated in Figure 1, as “a Randles–Sevcik voltammogram”. Semiintegration of this voltammogram produces a symmetrical function of sigmoidal shape, described by a much simpler formula, eq 16. Sigmoids of this shape, which is also illustrated in Figure 1, arise in many other voltammetric contexts and will be described here as “a standard sigmoid”.

Barker and Jenkins<sup>5</sup> were the first to modulate a ramp signal by adding a symmetrical square wave.<sup>6</sup> Fifty years later, a thorough investigation of this electrochemical approach was carried out by Gavaghan et al.<sup>7</sup> By simulation, the latter researchers examined the effects of the square-wave frequency and amplitude, confirming their predictions by voltammetric experiments with the ferrocene/ferricinium couple. Inasmuch as a square wave can be considered as a combination of sine waves of frequencies that are odd multiples of a fundamental frequency  $\omega$ , the prime focus of that study was to identify the amplitudes and phase angles of the reversible current components of frequencies  $\omega$ ,  $3\omega$ ,  $5\omega$ , ... and to decipher how these how are influenced by the dc potential. In addition, these

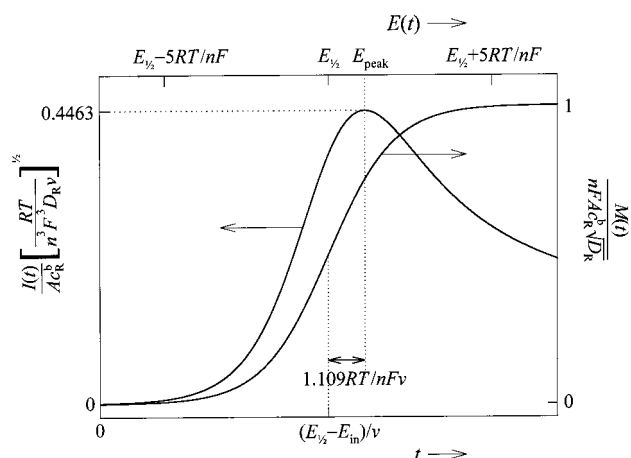


**Figure 1.** The standard Randles–Sevcik voltammogram and its semiintegrated counterpart.

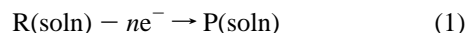
workers extracted from their simulations the effect that the square-wave modulation had upon the dc current signal, observing an intriguing “splitting effect”.

The purpose of the present short article is to demonstrate that a rigorous mathematical analysis can generate the same information as that found by the simulations of Gavaghan et al.<sup>7</sup> and to elaborate on the implications. The results of the two approaches are compared in a later section.

The procedure followed here is first to deduce the semiintegral of the current and then semidifferentiate this to find the current itself. A similar route was followed by Engblom et al.<sup>8</sup> in their treatment of reversible ac voltammetry. It will transpire that the formulas for the dc and ac components of the current in square-wave-modulated linear-potential-scan voltammetry are very simple indeed, surprisingly being less complex than when the modulating wave is sinusoidal.

## General Derivation

We consider the reversible reaction



proceeding at a planar working electrode in an electrolyte

\* To whom correspondence should be addressed. E-mail: KOldham@TrentU.CA. Tel: 705-748-1011x1336. Fax: 705-748-1625.

† Permanent address: Trent University, Peterborough, Canada K9J 7B8.

‡ Permanent address: Oxford University Computing Laboratory, Wolfson Bldg, Parks Rd., Oxford OX1 3QD, England.

solution that contains a bulk concentration  $c_R^b$  of the reactant, R, but that is initially devoid of the product, P. The electron number,  $n$ , may have either sign, so that oxidations or reductions are covered equally by the treatment. The presence of excess supporting electrolyte, the quiescence of the solution, and the relatively large area,  $A$ , of the electrode conspire to ensure that the reaction proceeds under conditions in which planar semi-infinite diffusion governs the transport of R and P. Initially, the electrode is held at a potential,  $E_{in}$ , sufficiently extreme that reaction 1 occurs negligibly. Starting at time  $t = 0$ , the electrode is subjected to a time-varying potential that contains both a dc and an ac component, the former being a simple ramp:

$$E(t) = E_{dc} + E_{ac} = E_{in} + \nu t + E_{ac}(t) \quad (2)$$

where  $\nu$ , which shares the sign of  $n$ , is a rather slow sweep rate. Because the electron-transfer reaction is taken to be reversible, the concentrations of the reactant and product at the surface of the working electrode are linked by the Nernstian relationship

$$\frac{c_P^s(t)}{c_R^s(t)} = \exp\left\{\frac{nF}{RT}[E(t) - E^\circ]\right\} \quad (3)$$

where  $E^\circ$  is the conditional (or formal) potential of reaction 1 and the symbols  $F$ ,  $R$ , and  $T$  having their usual electrochemical meanings. Under the prescribed condition of semiinfinite planar diffusion, it is well-known that the volumetric surface concentrations of R and P are also related to each other and to the Faradaic current through the equations

$$\sqrt{D_R}[c_R^b - c_R^s(t)] = \frac{M(t)}{nFA} = \sqrt{D_P}c_P^s(t) \quad (4)$$

where  $D_R$  and  $D_P$  are diffusivities (or diffusion coefficients).  $M(t)$  is the semiintegral of Faradaic current,  $I(t)$ , to which it is linked via the integral transform

$$M(t) = \frac{1}{\sqrt{\pi}} \int_0^t \frac{I(Y)}{\sqrt{t-Y}} dY \quad (5)$$

That the bulk concentration of P is zero is incorporated into relationship 4.

Equations 4 and 3 may be combined into

$$\frac{2M(t)}{nFA\sqrt{D_R}c_R^b} = \frac{1}{1 + \exp\left\{\frac{nF}{RT}[E(t) - E_{1/2}]\right\}} \quad (6)$$

where  $E_{1/2}$ , the half-wave potential, is defined by

$$E_{1/2} = E^\circ + \frac{RT}{2nF} \ln\left\{\frac{D_P}{D_R}\right\} \quad (7)$$

When eq 2 is now incorporated into eq 6, one finds

$$\frac{2M(t)}{nFA\sqrt{D_R}c_R^b} = 1 + \tanh\left\{\frac{nF}{2RT}[E_{in} - E_{1/2} + \nu t + E_{ac}(t)]\right\} \quad (8)$$

after replacement of the exponential function by a hyperbolic tangent of half-argument. This equation is valid for a reversible reaction irrespective of the nature of the ac signal. With  $E_{ac}(t) = V \sin(\omega t)$ , for example, it was the basis of a study of ac voltammetry by Engblom and co-workers.<sup>8</sup> Here, however, we shall treat the case in which the ac part of the applied signal is

a symmetrical square wave of amplitude  $\Delta E$  and period  $P$ , as in the upper panel of Figure 3 below. This can be represented concisely by a representation that employs  $\text{Int}\{\}$ , the integer-value function;<sup>9</sup> thus,

$$E_{ac}(t) = (-)^{\text{Int}\{2t/P\}} \Delta E \quad (9)$$

Alternatively, one can represent  $E_{ac}(t)$  as  $(-)^{\text{Int}\{\omega t/\pi\}} \Delta E$  where  $\omega$  is the angular frequency, equal to  $2\pi/P$ , ascribable to the square wave.

It is convenient to adopt the definitions

$$\xi_{dc} = \frac{nF[E_{dc} - E]}{2RT} = \frac{nF[E_{in} - E_{1/2} + \nu t]}{2RT} \quad (10)$$

$$\Delta\xi = \frac{nF\Delta E}{2RT} \quad (11)$$

and

$$\xi_{ac} = \frac{nFE_{ac}(t)}{2RT} = (-)^{\text{Int}\{2t/P\}} \Delta\xi \quad (12)$$

whereby eq 8 becomes

$$\frac{2M(t)}{nFA\sqrt{D_R}c_R^b} = 1 + \tanh\{\xi_{dc} + \xi_{ac}\} = 1 + \tanh\{\xi_{dc} + (-)^{\text{Int}\{2t/P\}} \Delta\xi\} \quad (13)$$

In an appendix, we show that this may be rewritten

$$\frac{2M(t)}{nFA\sqrt{D_R}c_R^b} = 1 + \frac{1}{2} \tanh\{\xi_{dc} - \Delta\xi\} + \frac{1}{2} \tanh\{\xi_{dc} + \Delta\xi\} + \frac{1}{2} (-)^{\text{Int}\{2t/P\}} [\tanh\{\xi_{dc} + \Delta\xi\} - \tanh\{\xi_{dc} - \Delta\xi\}] \quad (14)$$

Evident in this equation is that the semiintegral of the current decomposes naturally into dc and ac components, which we shall examine separately. First, however, it is propitious to review the properties of the response to the unmodulated ramp.

### The Unmodulated Response

The reversible current,  $I$ , flowing in response to a linear-potential scan may be considered as a function of time,  $t$ , or as a function of the potential,  $E$ . Because these latter two variables are linearly interrelated, we may profitably replace either by the dimensionless variable  $\xi_{dc}$  defined by eq 10. With this quantity as the independent variable, the equation describing the current is the Randles-Sevcik formula<sup>4</sup>

$$I_{rs}(\xi_{dc}) = \frac{Ac_R^b}{4} \sqrt{\frac{\pi n^3 F^3 D_R \nu}{RT}} \sum_{j=1,3}^{\infty} \frac{\sqrt{\Xi - \xi_{dc}(\Xi + 2\xi_{dc})}}{\Xi^3} \quad (15)$$

where  $\Xi = \sqrt{(j^2 \pi^2/4) + \xi_{dc}^2}$ . This, then, is the equation of the Randles-Sevcik voltammogram. Equations 15 and 16 were used to generate Figure 1.

Semiintegration of eq 15 produces the supremely simple result

$$M_{rs}(\xi_{dc}) = \frac{nFA\sqrt{D_R}c_R^b}{2} [1 + \tanh\{\xi_{dc}\}] \quad (16)$$

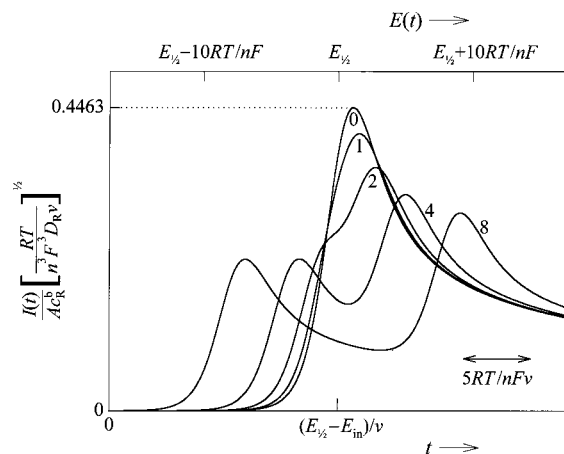


**Figure 2.** The shape of the dc current component in square-wave-modulated linear-potential-scan voltammetry for various amplitudes of the square-wave modulation. The number attaching to each curve is  $nF\Delta E/(RT)$ .

which describes the standard (Randles–Sevcik) sigmoid. Historically, the converse procedure was followed,<sup>10</sup> eq 15 being deduced by semidifferentiation of eq 16. Notice that, unlike the Randles–Sevcik current, the sigmoid is independent of the scan rate,  $v$ .

### The dc Component of the Modulated Response

The first three right-hand terms in eq 14, which it is convenient to rewrite as

$$M_{dc} = \frac{nFA\sqrt{D_R c_R^b}}{2} \left[ \frac{1}{2} (1 + \tanh\{\xi_{dc} - \Delta\xi\}) + \frac{1}{2} (1 + \tanh\{\xi_{dc} + \Delta\xi\}) \right] \quad (17)$$

constitute the semiintegrated dc component of the square-wave-modulated linear-potential-scan voltammogram. Again, the response is expressed in terms of the variable  $\xi_{dc}$ , which may be considered as a dimensionless analogue of either dc potential or time. When  $\Delta\xi = 0$ , i.e., when there is no modulation, the semiintegral reduces to the standard sigmoid, eq 16, as expected.

On comparing eq 17, which applies when there is square-wave modulation, with eq 16, applicable when modulation is absent, one notices that

$$M_{dc}(\xi_{dc}) = \frac{M_{rs}(\xi_{dc} - \Delta\xi) + M_{rs}(\xi_{dc} + \Delta\xi)}{2} \quad (18)$$

It follows that a similarly simple relationship, namely,

$$I_{dc}(\xi_{dc}) = \frac{I_{rs}(\xi_{dc} - \Delta\xi) + I_{rs}(\xi_{dc} + \Delta\xi)}{2} \quad (19)$$

applies to the currents themselves. To state this remarkable relationship in words, *the dc voltammogram of a square-wave-modulated ramp experiment is the average of two Randles–Sevcik voltammograms, one shifted to positive potentials by  $nF\Delta E/(2RT)$  and the other shifted negatively by the same amount.* This unexpected behavior, which is illustrated in Figure 2, was reported as an empirical observation, the “splitting effect”, by Gavaghan et al.<sup>7</sup> based on both simulation and experiment. A rationale for this behavior is presented in Figure 3. The modulated ramp can be regarded as two ramps, initiating

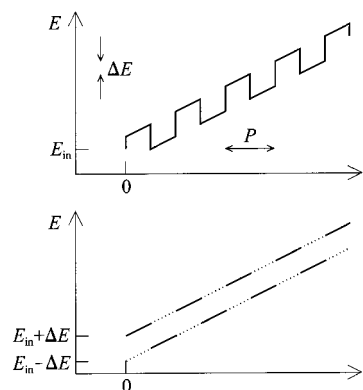


**Figure 3.** The square-wave-modulated ramp, shown in the upper panel, can be resolved into two parallel ramps, as shown in the lower panel, each active for half of the time.

at potentials  $E_{in} - \Delta E$  and  $E_{in} + \Delta E$ , each being active for one-half of the time.

### The ac Component of the Modulated Response

Equation 14 shows that square-wave modulation of the applied potential results in the appearance of the ac component

$$M_{ac}(\xi_{dc}, t) = (-)^{\text{Int}\{2t/P\}} \frac{nFA\sqrt{D_R c_R^b}}{4} [\tanh\{\xi_{dc} + \Delta\xi\} - \tanh\{\xi_{dc} - \Delta\xi\}] \quad (20)$$

in the semiintegral of the current. Thus, the ac semiintegral is itself a square wave with the same periodicity as the applied modulation and of an amplitude that depends on the dc potential and on the square wave’s amplitude but not on the frequency of the square wave. When we rewrite this expression as

$$\frac{2M_{ac}(\xi_{dc}, t)}{nFA\sqrt{D_R c_R^b}} = (-)^{\text{Int}\{2t/P\}} \left( \frac{1}{2} [1 + \tanh\{\xi_{dc} + \Delta\xi\}] - \frac{1}{2} [1 + \tanh\{\xi_{dc} - \Delta\xi\}] \right) \quad (21)$$

and compare it with eq 16, it becomes clear that the amplitude of the ac component of the modulated voltammogram is proportional to the *difference* of two standard sigmoids. In fact,

$$M_{ac}(\xi_{dc}, t) = (-)^{\text{Int}\{2t/P\}} \frac{M_{rs}(\xi_{dc} + \Delta\xi) - M_{rs}(\xi_{dc} - \Delta\xi)}{2} \quad (22)$$

Figure 4 and its legend give an interpretation of this behavior. The maximum value of  $M_{ac}$  occurs when  $\xi_{dc}$  is zero, i.e., at the half-wave potential. There,

$$M_{ac}(E_{1/2}, t) = (-)^{\text{Int}\{2t/P\}} \frac{nFA\sqrt{D_R c_R^b}}{4} \tanh\{\Delta\xi\} \quad (23)$$

The ac current can be found by semidifferentiation of eq 22. This does not affect the  $[M_{rs}(\xi_{dc} + \Delta\xi) - M_{rs}(\xi_{dc} - \Delta\xi)]/2$  term present in eq 22, which reflects how the ac component depends on the dc potential and on the amplitude of the square wave. The similarity between eqs 18 and 22, expressing respectively the dc and ac responses, is remarkable. In words, eq 22 or its semiderivative asserts that *the height of the ac voltammogram from a square-wave-modulated ramp experiment is proportional to the difference of two standard sigmoids, one*

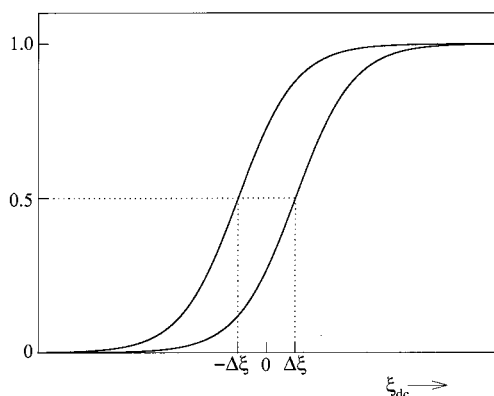


**Figure 4.** Two standard sigmoids differing in that their half-wave points lie at  $E_{1/2} - \Delta E$  and  $E_{1/2} + \Delta E$ . The two partial ramps shown in the lower panel of Figure 3 can be considered to give rise to these curves. The dc component of the current in square-wave-modulated linear-potential-scan voltammetry arises from semidifferentiating the sum of these two sigmoids, whereas the ac component arises directly from their difference.

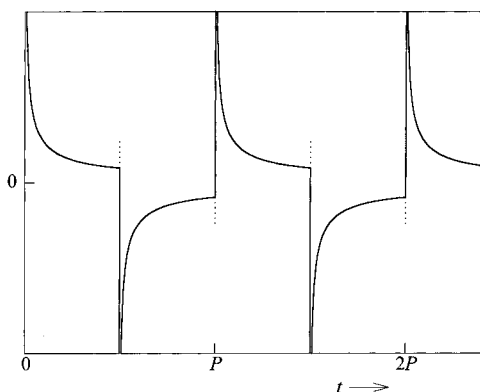


**Figure 5.** The semiderivative of a square wave. Dotted lines indicate “counterspikes” that were present in an experimental study,<sup>7</sup> which are not predicted theoretically.

shifted to positive potentials by  $nF\Delta E/(2RT)$  and the other shifted negatively by the same amount.

The semiderivative of a square wave of unit amplitude and period  $P$  is<sup>11</sup>

$$\sqrt{\frac{4}{\pi P}} \left[ \zeta \left\{ \frac{1}{2}; \text{frac} \left( \frac{t}{P} \right) \right\} - \zeta \left\{ \frac{1}{2}; \text{frac} \left( \frac{t}{P} + \frac{1}{2} \right) \right\} \right] \quad (24)$$

where  $\zeta \{ \frac{1}{2}; \}$  denotes a Hurwitz function<sup>11</sup> of moiety order. The  $\text{frac}()$  symbol signifies the fractional part of its argument;<sup>9</sup> it is the complement of the  $\text{Int}\{ \}$  function. Figure 4 shows the shape of a semidifferentiated square wave. It is a spiky periodic function that takes the value  $\infty$  at  $t = 0, P, 2P, 3P, \dots$ . The value declines toward<sup>12</sup>  $0.97/P^{1/2}$  as  $t$  approaches  $P/2, 3P/2, 5P/2, \dots$ , then suddenly jumps to  $-\infty$  when these midperiod values are attained, and thereafter climbs back toward  $-0.97/P^{1/2}$  as integer values of  $t/P$  are again approached. This description does not precisely match the shapes found experimentally by Gavaghan et al.,<sup>7</sup> which showed small additional spikes as illustrated in Figure 5, but the broad pattern was similar. One can assign the mean of its absolute value to be the “amplitude” of this semidifferentiated square wave. On this basis, the amplitude of the semiderivative of a square wave of period  $P$  and unity amplitude can be shown to be<sup>13</sup>  $2.43P^{-1/2}$ .

Semidifferentiation of eq 22 gives<sup>14</sup>

$$\begin{aligned} I_{ac}(\xi_{dc}, t) &= \sqrt{\frac{2}{\pi P}} \left[ \zeta \left\{ \frac{1}{2}; \text{frac} \left( \frac{t}{P} \right) \right\} - \zeta \left\{ \frac{1}{2}; \text{frac} \left( \frac{t}{P} + \frac{1}{2} \right) \right\} \right] [M_{rs}(\xi_{dc} + \Delta\xi) - M_{rs}(\xi_{dc} - \Delta\xi)] \\ &= \left[ \zeta \left\{ \frac{1}{2}; \text{frac} \left( \frac{t}{P} \right) \right\} - \zeta \left\{ \frac{1}{2}; \text{frac} \left( \frac{t}{P} + \frac{1}{2} \right) \right\} \right] \frac{nFAc_R^b}{4} \sqrt{\frac{D_R}{\pi P}} [\tanh\{\xi_{dc} + \Delta\xi\} - \tanh\{\xi_{dc} - \Delta\xi\}] \quad (25) \end{aligned}$$

This gives a complete theoretical description of the ac response in the square-wave-modulated linear-potential-scan voltammetry. The amplitude of the ac response is greatest at the half-wave potential, being

$$I_{ac}(\xi_{dc}=0, t) = \left[ \zeta \left\{ \frac{1}{2}; \text{frac} \left( \frac{t}{P} \right) \right\} - \zeta \left\{ \frac{1}{2}; \text{frac} \left( \frac{t}{P} + \frac{1}{2} \right) \right\} \right] \frac{nFAc_R^b}{2} \sqrt{\frac{D_R}{\pi P}} \tanh\{\Delta\xi\} \quad (26)$$

at that point where  $\xi_{dc}$  vanishes.

Another approach is to embrace a frequency-domain description of the square wave by ascribing it a frequency  $\omega$  equal to  $2\pi/P$ . Then, as an alternative to eq 9, the ac perturbation may be represented by an infinite Fourier series containing only the fundamental frequency  $\omega$  and its odd harmonics:

$$E_{ac}(t) = (-)^{\text{Int}\{\omega t/\pi\}} \Delta E = \frac{4\Delta E}{\pi} \sum_{k=1,3}^{\infty} \frac{\sin\{k\omega t\}}{k} \quad (27)$$

The response to the modulated ramp may then be described, as in eq 22, by

$$M_{ac}(\xi_{dc}, t) = \frac{2}{\pi} [M_{rs}(\xi_{dc} + \Delta\xi) - M_{rs}(\xi_{dc} - \Delta\xi)] \sum_{k=1,3}^{\infty} \frac{\sin\{k\omega t\}}{k} \quad (28)$$

which, after semidifferentiation, leads to the ac current response being

$$I_{ac}(\xi_{dc}, t) = \frac{nFAc_R^b}{\pi} \sqrt{D_R \omega} [\tanh\{\xi_{dc} + \Delta\xi\} - \tanh\{\xi_{dc} - \Delta\xi\}] \sum_{k=1,3}^{\infty} \frac{\sin\{k\omega t + \pi/4\}}{\sqrt{k}} \quad (29)$$

as an alternative representation of eq 25 showing the restriction to *odd* harmonics and the  $45^\circ$  phase shift. The  $\xi_{dc} = 0$  version of this equation, namely,

$$I_{ac}(\xi_{dc}=0, t) = \frac{2nFAc_R^b}{\pi} \sqrt{D_R \omega} \tanh\{\Delta\xi\} \sum_{k=1,3}^{\infty} \frac{\sin\{k\omega t + \pi/4\}}{\sqrt{k}} \quad (30)$$

was published earlier.<sup>15</sup> Notice in eq 29 that all of the harmonics depend in exactly the same way on the dc potential and the square-wave amplitude, differing only by the presence of the  $k^{-1/2}$  multiplier, where  $k = 1, 3, 5, \dots$ , even harmonics being totally absent. This situation is dramatically different from linear-potential-scan voltammetry with sine-wave modulation,<sup>16</sup> in which harmonics at *all* multiples of  $\omega$  are present, each with its own individual dependence on  $\xi_{dc}$  and  $\Delta\xi$ .



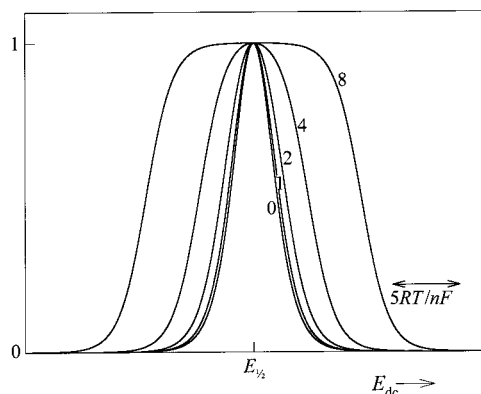


**Figure 6.** Shapes of the ac component of square-wave-modulated linear-potential-scan voltammograms for the values of  $nF\Delta E/(RT)$  shown, where  $\Delta E$  is the square-wave amplitude.

The “shape” of the ac component of the modulated voltammogram, i.e., the form of the dependence of the ac current on the parameters  $\xi_{dc}$  and  $\Delta\xi$ , is the same for each of the  $k\omega$  harmonics ( $k = 1, 3, 5, \dots$ ) as it is for the current as a whole. The maximum occurs at  $\xi_{dc} = 0$ ; that is at the half-wave potential, as given in eq 26 in the time domain representation or in eq 30 in the language of the frequency. At other dc potentials, the signal is less than the maximal signal by the factor

$$\frac{I_{ac}(\xi_{dc})}{I_{ac}(\xi_{dc}=0)} = \frac{\tanh\{\xi_{dc} + \Delta\xi\} - \tanh\{\xi_{dc} - \Delta\xi\}}{2 \tanh\{\Delta\xi\}} \quad (31)$$

Plots of this function, for various values of  $\Delta E$ , are displayed in Figure 6.

As the figure shows, the shape of the peak changes as  $\Delta E$  increases, becoming flat-topped. The peak width at half-height is given by the general formula

$$W_{\text{peak}} \approx \frac{4RT}{nF} \operatorname{arsinh}\left\{\cosh\left(\frac{nF\Delta E}{2RT}\right)\right\} \quad (32)$$

but this simplifies if the square-wave amplitude,  $\Delta E$ , is either small or large. For small amplitudes, the peak shape is independent of  $\Delta E$  and has a width of

$$W_{\text{peak}} \approx \frac{4RT}{nF} \operatorname{arcosh}\{\sqrt{2}\} = \frac{91 \text{ mV}}{n} \quad \text{for} \quad \Delta E < \frac{RT}{2nF} = \frac{13 \text{ mV}}{n} \quad (33)$$

For large square-wave amplitudes, the peak width is proportional to the amplitude. In fact,

$$W_{\text{peak}} \approx 2\Delta E \quad \text{for} \quad \Delta E > \frac{4RT}{nF} = \frac{103 \text{ mV}}{n} \quad (34)$$

The approximations in expressions 33 and 34 allow for no more than 2% errors and the millivolts relate to  $T = 298 \text{ K}$ .

### Comparison with Another Study

The present study has produced analytical expressions for both the dc and the ac components of the current resulting from square-wave-modulated linear-potential-scan voltammetry. Each of these can be compared with the results of the Fourier transform simulation of Gavaghan et al.<sup>7</sup>

Figure 7 shows again the  $nF\Delta E/(RT) = 2$  curve from Figure 2 and compares it with numerical data generated by Gavaghan et al., which were themselves shown to concur with experiment.<sup>7</sup>

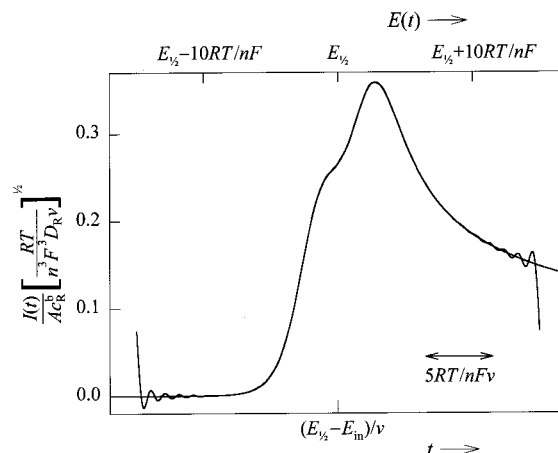


**Figure 7.** Comparison of the dc component of the square-wave-modulated linear-potential-scan voltammograms predicted by the analytical treatment of this study and that simulated by Gavaghan et al.<sup>7</sup> For both curves, the square-wave amplitude is  $2RT/(nF)$ . The analytical curve assumes remote initial and final potentials, whereas the span of the simulation is  $15RT/(nF)$  units either side of the half-wave potential.

**TABLE 1: Comparison of Widths, in Units of  $RT/(nF)$ , of Simulated ac Voltammetric Peaks with the Predictions of Eq 32<sup>a</sup>**

$nF\Delta E/(RT)$	eq 32	simulation <sup>7</sup>				
	all $k$	$k = 1$	$k = 2$	$k = 5$	$k = 10$	$k = 20$
0	3.5255					
0.10	3.53	3.53	3.53	3.53	3.54	3.53
1.00	3.88	3.88	3.88	3.88	3.88	3.88
2.00	4.87	4.87	4.87	4.87	4.87	4.88
4.00	8.14	8.14	8.14	8.14	8.14	8.14
8.00	16.00	16.00	16.00	16.00	16.00	16.00

<sup>a</sup>  $k$  denotes the harmonic number.

Notice that the curves virtually overlap, except at the extremes of the voltage range used in the simulation. The discrepancy is an artifact of the Fourier transform procedure. We use Table 1 to compare our prediction that the widths of the ac peaks are independent of the harmonic number,  $k$ , and given by formula 32.

### Discussion

It should be noted that the version of square-wave voltammetry discussed in this, and our previous, paper is quite different from the version that was invented by Ramaley and Krause<sup>17,18</sup> and popularized by the Osteryoungs and O'Dea.<sup>19,20</sup> The latter employs a square wave superimposed on a staircase as the applied potential waveform, while sampled and differenced currents provide the output. Here, we are concerned with a square wave that modulates a ramp, not a staircase, and the entire current, including the dc component, is regarded as the output signal. Processing into the frequency domain creates such a different milieu from that of Ramaley–Krause–Osteryoung–O'Dea voltammetry that comparisons between the two approaches are difficult to come to grips with. As here, Baranski and Szulborska<sup>21</sup> employed Fourier transformation in their application of square-wave voltammetry<sup>22</sup> to the measurement of the kinetics of electrode processes, but their treatment was limited to square waves of small amplitude.

One advantage of our simple approach is the possibility, at least for reversible processes, of having an analytical solution in contrast to the computational evaluation that is mandatory

in the Osteryoung–O'Dea version. Clearly, the dangers of overlooking an anomaly are lessened, and noise suppressed, when the entire current is analyzed, rather than placing reliance on isolated points in the current spectrum. Those points are chosen strategically to maximize discrimination against charging current and are very successful in that regard. Discrimination based on phase angle is an effective alternative, commonly adopted in the frequency domain.

**Acknowledgment.** The authors are grateful for financial assistance from the Natural Sciences and Engineering Research Council of Canada, the Medical Research Council of Great Britain, and the Australian Research Council.

## Appendix

Let us adopt the temporary abbreviations  $S = \tanh\{\xi_{dc}\}$  and  $T = \tanh\{\Delta\xi\}$ . Then, the addition formula for the hyperbolic tangent function permits us to write

$$\begin{aligned} 1 + \tanh\{\xi_{dc} + (-)^{\text{Int}\{2t/P\}}\Delta\xi\} \\ = 1 + \frac{S + \tanh\{(-)^{\text{Int}\{2t/P\}}\Delta\xi\}}{1 + S \tanh\{(-)^{\text{Int}\{2t/P\}}\Delta\xi\}} \\ = 1 + \frac{S + (-)^{\text{Int}\{2t/P\}}T}{1 + (-)^{\text{Int}\{2t/P\}}ST} \quad (\text{A1}) \end{aligned}$$

the second step being valid because the hyperbolic tangent is an odd function. For finite real argument, the  $\tanh\{\}$  function always has a magnitude of less than unity, and therefore,  $-1 < (-)^{\text{Int}\{2t/P\}}ST < 1$ . Hence, we may binomially expand the denominatorial term above as

$$[1 + (-)^{\text{Int}\{2t/P\}}ST]^{-1} = \sum_{j=0}^{\infty} (-)^j [(-)^{\text{Int}\{2t/P\}}ST]^j \quad (\text{A2})$$

Raising  $(-)^{\text{Int}\{2t/P\}}$  to an even integer power produces +1, while raising  $(-)^{\text{Int}\{2t/P\}}$  to an odd integer power leaves  $(-)^{\text{Int}\{2t/P\}}$  unchanged. Thus, when we split the summation into two sums according to the parity of  $j$ , we find

$$[1 + (-)^{\text{Int}\{2t/P\}}ST]^{-1} = \sum_{j=0,2}^{\infty} S^j T^j + (-)^{\text{Int}\{2t/P\}} \sum_{j=1,3}^{\infty} S^j T^j \quad (\text{A3})$$

Being infinite geometric series, the summations are readily evaluated; whence,

$$[1 + (-)^{\text{Int}\{2t/P\}}ST]^{-1} = [1 - (-)^{\text{Int}\{2t/P\}}ST][1 - S^2T^2]^{-1} \quad (\text{A4})$$

Accordingly, by returning to the first equation of this appendix,

$$\begin{aligned} 1 + \tanh\{\xi_{dc} + (-)^{\text{Int}\{2t/P\}}\Delta\xi\} \\ = 1 + \frac{[S + (-)^{\text{Int}\{2t/P\}}T][1 - (-)^{\text{Int}\{2t/P\}}ST]}{1 - S^2T^2} \quad (\text{A5}) \end{aligned}$$

On collecting terms that do, or do not, contain the  $(-)^{\text{Int}\{2t/P\}}$  factor, one discovers that

$$\begin{aligned} 1 + \tanh\{\xi_{dc} + \xi_{ac}\} = 1 + S \frac{1 - T^2}{1 - S^2T^2} + \\ (-)^{\text{Int}\{2t/P\}} T \frac{1 - S^2}{1 - S^2T^2} \quad (\text{A6}) \end{aligned}$$

The right-hand term that multiplies  $(-)^{\text{Int}\{2t/P\}}$  can be partial-fractioned and condensed as follows

$$\begin{aligned} T \frac{1 - S^2}{1 - S^2T^2} &= \frac{S + T}{2(1 + ST)} - \frac{S - T}{2(1 - ST)} \\ &= \frac{\tanh\{\xi_{dc} + \Delta\xi\}}{2} - \frac{\tanh\{\xi_{dc} - \Delta\xi\}}{2} \quad (\text{A7}) \end{aligned}$$

Similarly

$$\begin{aligned} 1 + S \frac{1 - T^2}{1 - S^2T^2} \\ = 1 + \frac{S - T}{2(1 - ST)} + \frac{S + T}{2(1 + ST)} \\ = \frac{1 + \tanh\{\xi_{dc} - \Delta\xi\}}{2} + \frac{1 + \tanh\{\xi_{dc} + \Delta\xi\}}{2} \quad (\text{A8}) \end{aligned}$$

These results establish eq 14 of the main text.

## References and Notes

- (1) Randles, J. E. B. *Trans. Faraday Soc.* **1948**, *44*, 327.
- (2) Sevcik, A. *Collect. Czech. Chem. Commun.* **1948**, *3*, 349.
- (3) Nicholson, R. S.; Shain, I. *Anal. Chem.* **1964**, *36*, 706.
- (4) Oldham, K. B. *J. Electroanal. Chem.* **1979**, *105*, 373.
- (5) Barker, G. C.; Jenkins, I. L. *Analyst* **1952**, *77*, 685.
- (6) They used a square wave of amplitude 6 mV and of period 4.44 ms.
- (7) Gavaghan, D. J.; Elton, D.; Oldham, K. B.; Bond, A. M. *J. Electroanal. Chem.*, in press.
- (8) Engblom, S. O.; Myland, J. C.; Oldham, K. B. *J. Electroanal. Chem.* **2000**, *480*, 120.
- (9) Spanier, J.; Oldham, K. B. *An Atlas of Functions*; Hemisphere: Washington, 1987; Chapter 9.
- (10) Oldham, K. B. *SIAM J. Math. Anal.* **1983**, *14*, 974.
- (11) Spanier, J.; Oldham, K. B. *An Atlas of Functions*; Hemisphere: Washington, 1987; Chapter 64.
- (12) The exact value is  $2(\pi P)^{-1/2}[2^{1/2} - 2]\zeta(1/2) = 0.965\,278\,58/P^{1/2}$ , with  $\zeta(\ )$  denoting Riemann's zeta function, some values of which have been tabulated in: Oldham, K. B. *SIAM J. Math. Anal.* **1970**, *1*, 538.
- (13) The exact value is  $16(\pi P)^{-1/2}[2^{-1/2} - 2]\zeta(-1/2) = 2.426\,238\,03/P^{1/2}$ .
- (14) In carrying out this operation, the  $[M_{rs}(\xi_{dc} + \Delta\xi) - M_{rs}(\xi_{dc} - \Delta\xi)]$  term was treated as constant. Strictly, it is a weak function of time by virtue of the time-dependence of  $\xi_{dc}$ . Provided  $vP \ll RT/(nF)$ , as is usual in experimental practice, the neglect of this time dependence will not introduce a significant error.
- (15) Equation 27 in ref 7.
- (16) Gavaghan, D. J.; Bond, A. M. *J. Electroanal. Chem.* **2000**, *480*, 133.
- (17) Ramaley, L.; Krause, M. S. *Anal. Chem.* **1969**, *41*, 1362.
- (18) Krause, M. S.; Ramaley, L. *Anal. Chem.* **1969**, *41*, 1365.
- (19) Osteryoung, J. G.; O'Dea, J. J. In *Electroanalytical Chemistry*; Bard, A. J., Ed.; Dekker: New York, 1986; Volume 14, p 209.
- (20) O'Dea, J. J.; Osteryoung, J. G.; Osteryoung, R. A. *J. Phys. Chem.* **1983**, *87*, 21.
- (21) Baranski, A.; Szulborska, A. *J. Electroanal. Chem.* **1994**, *374*, 157.
- (22) Though these authors modulated a staircase, they used many square waves on each "tread" of the staircase, so the waveform could properly be regarded as a periodic signal plus a constant dc.